CHEMBIOCHEM

DOI: 10.1002/cbic.200700762

Boolean Logic Gates that Use Enzymes as Input Signals

Guinevere Strack, Marcos Pita, Maryna Ornatska, and Evgeny Katz*[a]

Biochemical systems that demonstrate the Boolean logic operations AND, OR, XOR, and InhibA were developed by using soluble compounds, which represent the chemical "devices", and the enzymes glucose oxidase (GOx), glucose dehydrogenase (GDH), alcohol dehydrogenase (AlcDH), and microperoxidase-11 (MP-11), which operated as the input signals that activated the logic gates. The enzymes were used as soluble materials and as immobilized biocatalysts. The studied systems are proposed to be a step towards the construction of "smart" signal-responsive materials with built-in Boolean logic.

Introduction

Computing performed by chemical systems upon variations of concentrations of reactive species is a novel direction in unconventional computing.[1,2] Chemical systems have been used to perform different computing operations that mimic various electronic elements, such as logic gates,[3,4] switches,[5,6] and memory units.[7,8] Computing operations have previously been performed by chemical reactions that proceed in solutions[9,10] or at chemically modified interfaces.[11] Variation of different physical parameters, such as light,[12–14] magnetic field,[15] electrical potential,[16,17] or changes in chemical compositions, for example, pH changes,[18] have been used to switch the states of the molecular systems and activate various computing operations. Chemical systems were assembled in "devices" that performed simple arithmetic operations (half-adder and half-subtractor[4,19–21]), and mimicked electronic units (digital demultiplexer[22] and keypad lock[23]). Further increases in complexity of the chemical computing systems resulted in the integration of single-functional "devices" in complex multifunctional computing networks.[24–26] Chemical systems can solve computing problems at the level of a single molecule;[27] this results in nanoscale computing units[28] and allows parallel computation by numerous molecules involved in various reactions.[29] Despite the fact that chemical computing is a very rapidly developing area of research, the field is still in a very early experimental and theoretical stage; however, a great future potential is expected.[30] Computing performed by biomolecular systems (biocomputing)[31] is one of the most promising branches in unconventional chemical computing because of the complexity of biological materials and their unique properties, such as selectivity of biocatalyzed reactions and specificity of biorecognition processes. The biocomputing systems could include DNA,[32] proteins,[33] immunorecognition pairs,[34] and whole cells.[35]

Recently developed enzyme-based logic gates[36–38] utilize the specificity of enzymatic biocatalytic reactions to allow multiple simultaneous reactions that proceed in one solution without interference and "cross-talk" between them. This has allowed the assembly of computing "devices" (half-adder and half-subtractor[37]) and computing networks composed of many concatenated logic gates that operate simultaneously in solutions.[39] These logic gates were composed of soluble enzymes that operate as the molecular "devices" and accept corresponding substrates (e.g., glucose and H_2O_2) as chemical input signals. In order to generate digitally encoded output signals (the intensity of output signal "1" should be much higher than the intensity of output signal "0") the chemical input signals were applied at high concentrations (0.3 M). In the present work we have applied enzymes that operate as the input signals that activate the logic gates upon addition of catalytic quantities in the nanomolar range.

Results and Discussion

In all logic gates the spectral changes of the solutions above a certain threshold value were considered to be output signal "1", otherwise the output signal was considered to be "0". The spectral changes were induced by the reactions biocatalyzed by added enzymes (soluble or immobilized), which were considered to be the input signal "1". The absence of enzyme was considered to be the input signal "0", which would result in no spectral changes (output signal "0"), when both enzymes are absent (the input signals "0,0").

Logic gates that operate with soluble enzymes as the catalytic input signals: the AND logic gate

The AND logic gate was composed of a solution containing glucose, oxygen, and ABTS. The spectral changes in this solution originate from the biocatalyzed oxidation of ABTS; this results in increased absorbance in the range of $\lambda = 400$–440 nm.[40] This reaction proceeds only in the presence of MP-11 as the biocatalytic input signal and H_2O_2 as the oxidizer (Figure 1 A). However, H_2O_2 does not exist in the original composition of the gate, and it is produced in situ only upon oxidation

[a] G. Strack, Dr. M. Pita, Dr. M. Ornatska, Prof. E. Katz
Department of Chemistry and Biomolecular Science
Clarkson University
Potsdam NY 13699-5810 (USA)
Fax: (+1) 315-2686610
E-mail: ekatz@clarkson.edu

of glucose by O_2, which is biocatalyzed by GOx as the input signal. Thus, addition of any of two enzymes, either GOx or MP-11, separately (input signals "0,1" or "1,0") does not result in the oxidation of ABTS and does not yield absorbance change in the system. Only the addition of both biocatalytic input signals, GOx and MP-11 (input signals "1,1"), results in the formation of H_2O_2 and then in the oxidation of ABTS (Figure 1B). The optical output signal was the measured absorbance at $\lambda = 415$ nm, and it was considered as "0" when $\Delta A < 0.03$ and "1" when $\Delta A > 0.05$ (Figure 1C). The observed output signals correspond to the features of the AND logic gate (Figure 1D).

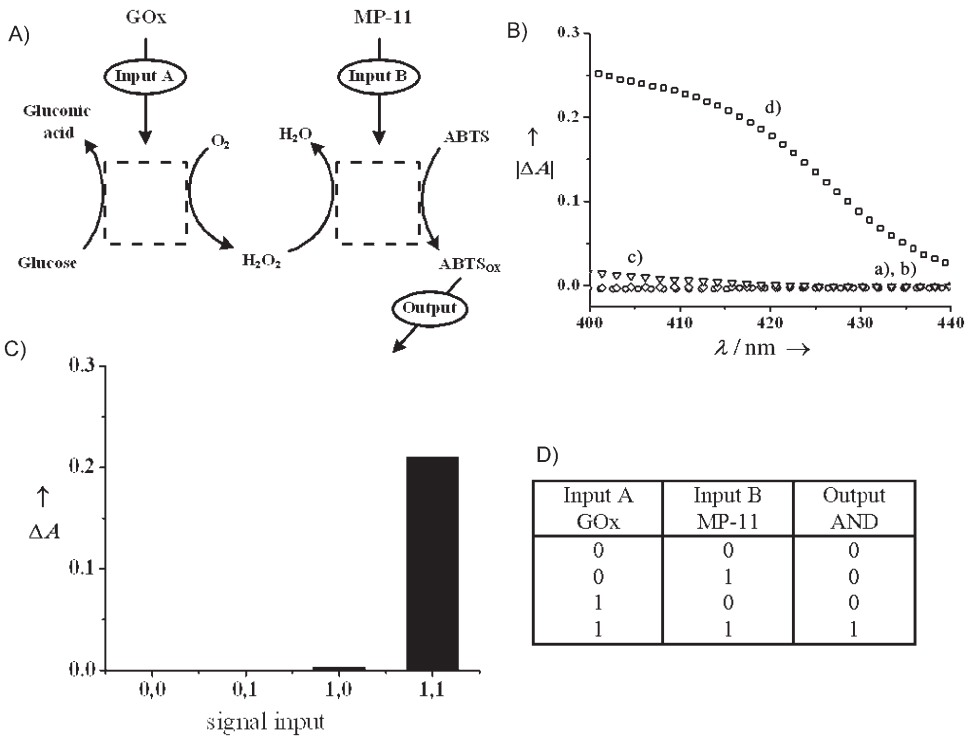

D)

Input A GOx	Input B MP-11	Output AND
0	0	0
0	1	0
1	0	0
1	1	1

Figure 1. The AND logic gate that operated with the soluble enzymes as the input signals. A) Schematic representation of the system. B) Spectra obtained 2 min after the input signals: a) "0,0": without additions of GOx or MP-11; b) "0,1": after the addition of MP-11 (5.4×10^{-7} M); c) "1,0": after the addition of GOx, (0.15 units); d) "1,1": after the addition of GOx (0.15 units) and MP-11 (5.4×10^{-7} M). C) Bar presentation of the AND gate absorbance outputs at $\lambda = 415$ nm. D) The truth table corresponding to the AND gate.

The OR logic gate

The OR logic gate was composed of NAD^+ cofactor and two reducing agents, glucose and ethanol. The spectral changes in this solution originate from the biocatalyzed reduction of NAD^+ to NADH (Figure 2A); this results in increased absorbance in the range of $\lambda =$ 300–370 nm.[41] This reaction proceeds in the presence of either of the two added enzymes—AlcDH operating with ethanol as the reductant (input signals "0,1") or GDH operating with glucose as the reductant (input signals "1,0")—or both of them together (input signals "1,1") to result in the formation of NADH and the associated absorbance increase (output signal "1"; Figure 2B). The optical output signal was measured as the absorbance at $\lambda = 340$ nm, and it was considered as "0" when $\Delta A < 0.1$ and "1" when $\Delta A > 0.2$ (Figure 2C). The observed output signals correspond to the features of the OR logic gate (Figure 2D).

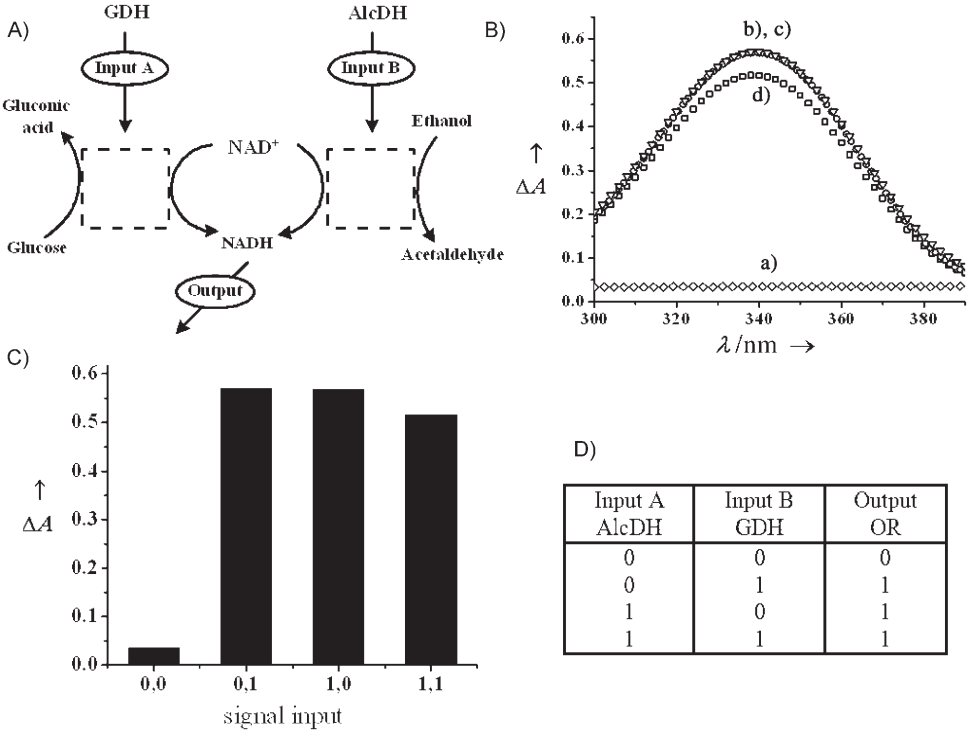

D)

Input A AlcDH	Input B GDH	Output OR
0	0	0
0	1	1
1	0	1
1	1	1

Figure 2. The OR logic gate that operated with soluble enzymes as the input signals. A) Schematic representation of the system. B) Spectra obtained 5 min after the input signals: a) "0,0": without additions of GDH or AlcDH; b) "0,1": after the addition of AlcDH (3.14 units); c) "1,0": after the addition of GDH (1.5 units); d) "1,1": after the addition of AlcDH (3.14 units) and GDH (1.5 units). C) Bar presentation of the OR gate absorbance outputs at $\lambda =$ 340 nm. D) The truth table corresponding to the OR gate.

The XOR logic gate

The XOR logic gate was composed of NADH, NAD^+, ethanol as the reductant, and H_2O_2 as the oxidant. The spectral changes in this solution originate from the biocatalyzed reduction of NAD^+ to NADH upon addition of the reducing enzyme AlcDH, or from the biocatalyzed oxidation of NADH upon addition of the oxidizing enzyme MP-11 to give increased or decreased absorbance in the range of $\lambda = 300$–370 nm,[41] respectively (Figure 3A). The oxidative reaction proceeds upon addition of MP-11 as the biocatalytic input (input signals "0,1"), and the reducing reaction proceeds upon addition of AlcDH as the biocatalytic input (input signals "1,0"); when the enzymes are added separately this results in a change in the absolute value of the absorbance. If both pathways, reductive and oxidative, are activated in the presence of both biocatalytic inputs (input signals "1,1") they compensate each other; this results in small optical changes in the system. It should be noted that the activities of both enzymes were optimized to provide similar reaction rates for both reactions. The optical output signal was measured as the absorbance at $\lambda = 340$ nm, and it was considered as "0" when $|\Delta A| < 0.15$ and "1" when $|\Delta A| > 0.2$ (Figure 3C). The observed output signals correspond to the features of the XOR logic gate (Figure 3D).

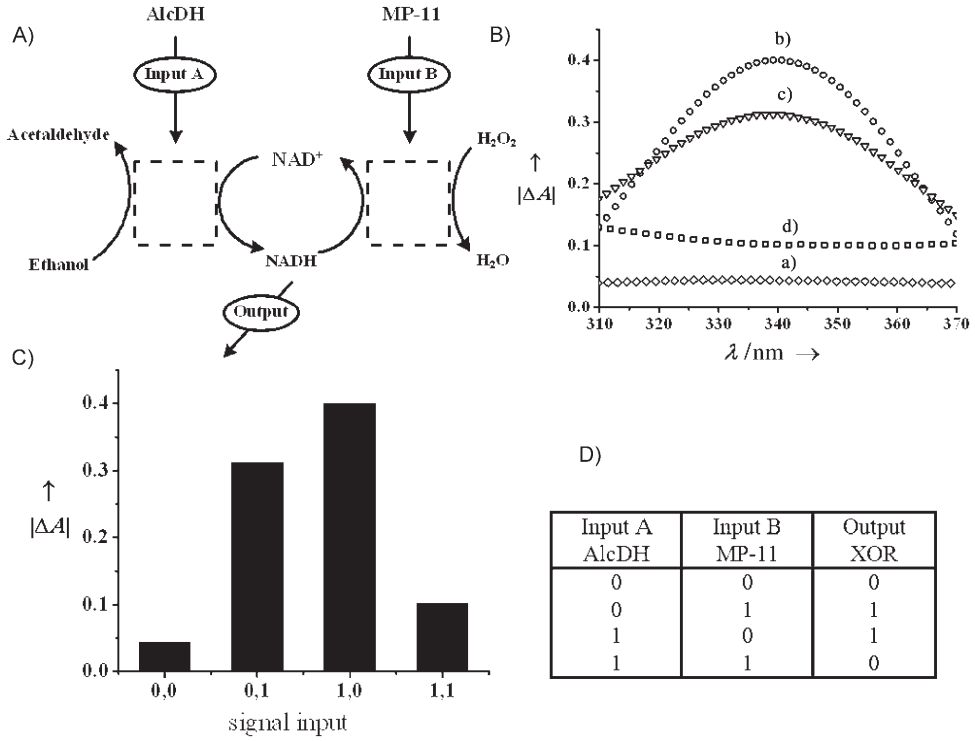

Input A AlcDH	Input B MP-11	Output XOR
0	0	0
0	1	1
1	0	1
1	1	0

Figure 3. The XOR logic gate that operated with soluble enzymes as the input signals. A) Schematic representation of the system. B) Spectra obtained 5 min after the input signals: a) "0,0": without additions of AlcDH and MP-11, b) "0,1": after the addition of MP-11 (5.4×10^{-7} M); c) "1,0": after the addition of AlcDH (3.14 units); d) "1,1": after the addition of AlcDH (3.14 units) and MP-11 (5.4×10^{-7} M). C) Bar presentation of the XOR gate absorbance outputs at $\lambda = 340$ nm. D) The truth table corresponding to the XOR gate.

The InhibA logic gate

The InhibA logic gate represents a modified version of the XOR gate, where the TRUE (1) output signal is converted to the FALSE (0) signal in the presence of the TRUE input signal in channel A (the InhibB logic gate can be constructed in a similar fashion). The InhibA logic gate was composed of NADH, ethanol as the reductant, and H_2O_2 as the oxidant. The spectral changes in this solution originate from the biocatalyzed oxidation of NADH upon addition of the oxidizing enzyme MP-11; this results in decreased absorbance in the range of $\lambda = 300$–370 nm[41] (Figure 4A). The addition of the reducing enzyme AlcDH as the input signal (input signals "0,1") does not result in any reaction because of the lack of the oxidized cofactor, NAD^+, in the system. The addition of the oxidizing enzyme MP-11 as the input signal (input signals "1,0") results in the oxidation of NADH and the respective decrease in absorbance. The addition of both enzymes, MP-11 and AlcDH (input signals "1,1") results in small changes in the system because the reductive pathway compensates the oxidative reaction and the NADH concentration and the respective absorbance remain unchanged (Figure 4B). It should be noted that the activity of the reducing enzyme AlcDH was selected so that it was much higher than the activity of MP-11; this kept the NADH cofactor reduced upon activation with both enzymes. The optical output signal was measured as the absorbance at $\lambda = 340$ nm, and it was considered as "0" when $|\Delta A| < 0.15$ and "1" when $|\Delta A| > 0.2$ (Figure 4C). The observed output signals correspond to the features of the InhibA logic gate (Figure 4D).

The AND logic gate that operated with immobilized enzymes as the catalytic input signals

Application of immobilized enzymes in different biotechnological systems is a well-known approach.[42] In the present study the biocatalysts, GOx and MP-11, were covalently bound to glass beads were used as the input signals to activate the AND logic gate. We also performed a similar modification procedure for the immobilization of the biocatalysts on silicon wafers, and used AFM and ellipsometry to characterize the modified surfaces. The biocatalytic film thicknesses derived from the el-

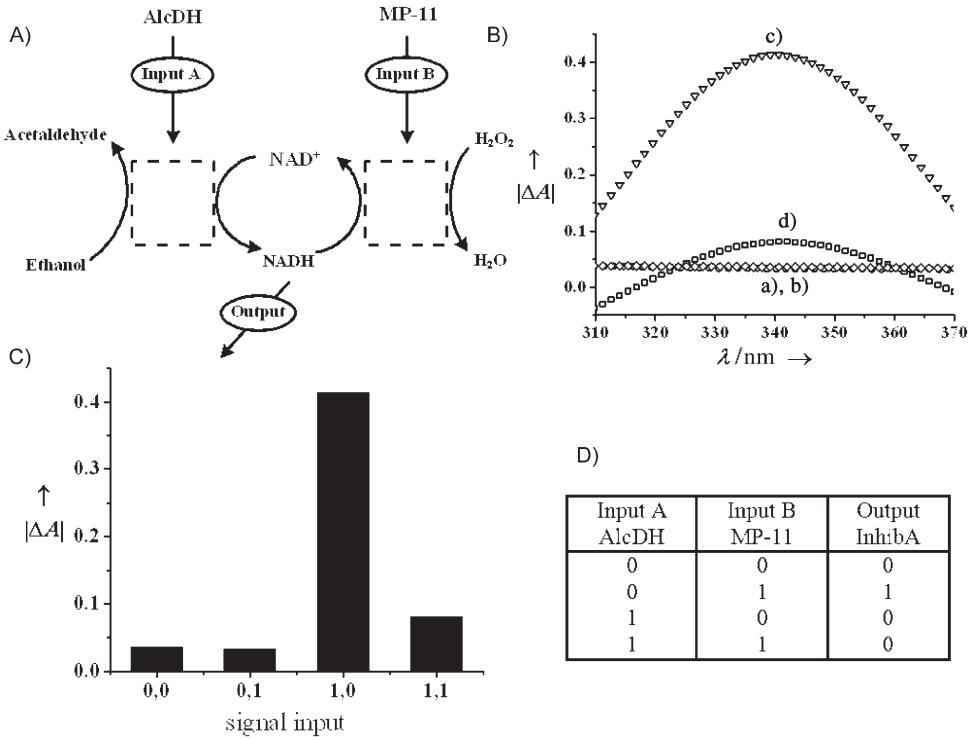

Input A AlcDH	Input B MP-11	Output InhibA
0	0	0
0	1	1
1	0	0
1	1	0

Figure 4. The InhibA logic gate that operated with the soluble enzymes as the input signals. A) Schematic representation of the system. B) Spectra obtained 5 min after the input signals: a) "0,0": without additions of AlcDH and MP-11, b) "0,1": after the addition of MP-11 (5.4×10^{-7} M); c) "1,0": after the addition of AlcDH (5.14 units); d) "1,1": after the addition of AlcDH (5.14 units) and MP-11 (5.4×10^{-7} M). C) Bar presentation of the XOR gate absorbance outputs at $\lambda = 340$ nm. D) The truth table corresponding to the XOR gate.

lipsometry were about 2.1 and 5.8 nm for the immobilized GOx and MP-11, respectively. If we compare the measured thicknesses to the molecular dimensions derived from the molecular models[43]—about 5 nm for GOx and about 1 nm for MP-11—the results indicate that GOx was deposited in a single monolayer that contained pinholes between the protein molecules, whereas MP-11 formed a multilayer assembly on the surface (about six layers of MP-11). High resolution AFM imaging showed dense surface coverage of GOx with the individual protein molecules visible as bright white spherical particles (Figure 5 A). The average diameter of these individual molecules was about 5 nm according to the cross-section analysis. The surface with the immobilized MP-11 layers shows high-density coverage (Figure 5 B); the morphology, however, points to the presence of molecular aggregates. Under the immobilization conditions used in the presence of EDC, MP-11 can form aggregates or polymers due to the cross-linking of the peptide fragments. The loading of GOx (about 0.1 pmol per bead) and MP-11 (about 30 pmol per bead) was calculated by using the biocatalyst film thicknesses derived from the ellipsometry measurements and by assuming that the same modification procedure results in similar coverage. The amount of GOx on the beads was also experimentally measured by hydrolyzing the biocatalyst and measuring the optical absorbance of the products; this gave the loading of about 0.4 pmol per bead. The experimentally observed GOx loading on the glass beads was about fourfold higher than the amount calculated from the ellipsometry measurements performed on a smooth solid support. This discrepancy originates from the rough surfaces of the glass beads.

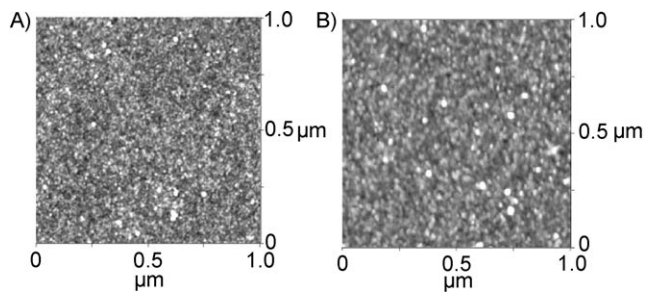

Figure 5. AFM tapping mode topography of: A) GOx and B) MP-11 immobilized on silica wafers.

The AND logic gate activated by the immobilized enzymes has the same composition and performance as described above for the soluble enzymes. The experimental results are shown in Figure 6, and they have similar explanations to the AND gate with the soluble enzyme inputs. It should be noted, however, that this system represents the first example of logic gates activated by immobilized enzymes and allows their multiple use as input signals.

Conclusions

The results presented here show that enzymes added to chemical systems as biocatalytic input signals can generate output signals that follow Boolean logic behavior. As a result of the high turnover of the biocatalytic inputs, meaningful changes in the systems could be obtained in the presence of small quantities of the enzyme inputs. The immobilized enzymes are able to generate the logic output signals in the chemical systems; they remain unchanged and ready for the next use. The enzyme-activated logic gates could be coupled with signal-responsive materials that operate as actuators controlled by the logic gate output signals. These "smart" materials will respond to two input signals that are converted by the logic gate into one output signal, which controls the properties of the material (e.g., porosity, density, absorbance, conductivity, etc.). The

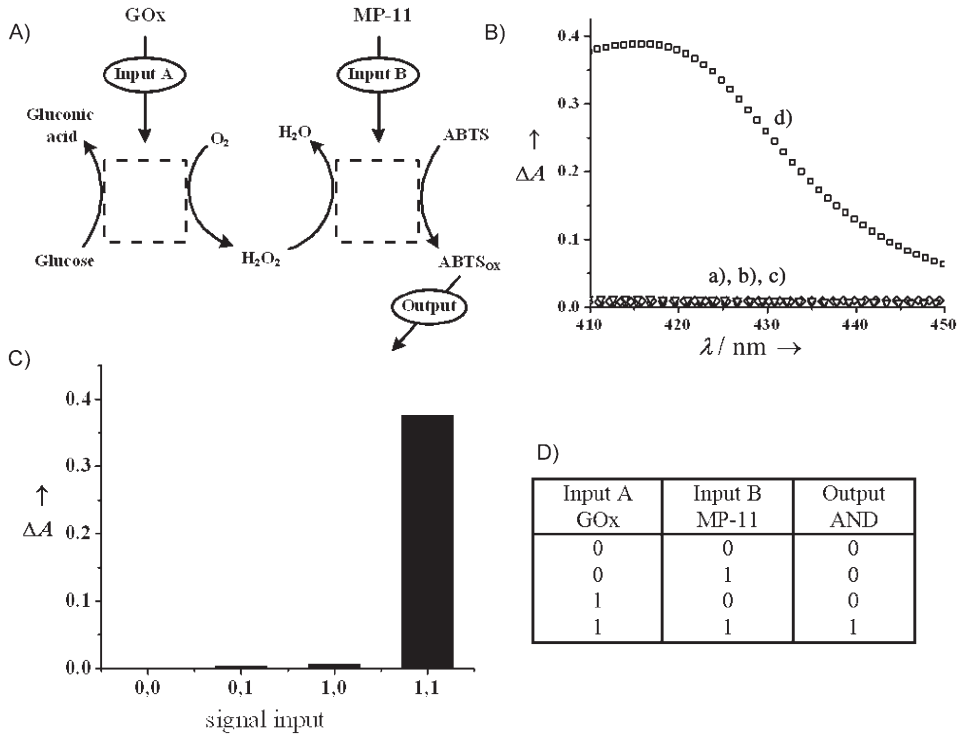

Input A GOx	Input B MP-11	Output AND
0	0	0
0	1	0
1	0	0
1	1	1

Figure 6. The AND logic gate that operated with the enzymes immobilized on glass beads as the input signals. A) Schematic representation of the system. B) Spectra obtained 10 min after the input signals: a) "0,0": without additions of GOx or MP-11, b) "0,1": after the addition of MP-11 (7.5 nmol); c) "1,0": after the addition of GOx (0.48 nmol); d) "1,1": after the addition of GOx (0.48 nmol) and MP-11 (7.5 nmol). C) Bar presentation of the AND gate absorbance outputs at $\lambda = 415$ nm. D) The truth table corresponding to the AND gate.

way in which the initial signals are converted to the final output signal will be controlled by the type of logic gate (e.g., AND, OR, XOR, InhibA). Multiple input signals that control the material properties will be possible upon assembling computing networks that are composed of many concatenated logic gates.[39] The integration of logic gates with various signal-responsive materials is underway in our laboratory.

Experimental Section

Chemicals and reagents: All enzymes were purchased from Sigma–Aldrich and were used as supplied. The enzymes that were used are: glucose oxidase (GOx) from *Aspergillus niger* type X-S (E.C. 1.1.3.4), alcohol dehydrogenase (AlcDH) from baker's yeast (*S. cerevisiae*; E.C. 1.1.1.1), glucose dehydrogenase (GDH) from *Pseudomonas* sp. (E.C. 1.1.1.47), and microperoxidase-11 (MP-11) prepared by enzymatic degradation of equine heart cytochrome c. All other chemicals (Sigma–Aldrich) were used without further purification: β-D-(+)-glucose, β-nicotinamide adenine dinucleotide (NAD^+), 1,4-dihydro-β-nicotinamide adenine dinucleotide (NADH), 4-(2-hydroxyethyl)piperazine-1-ethanesulfonic acid sodium salt (HEPES), 1-ethyl-3-(3-dimethylaminopropyl)carbodiimide (EDC), glutaric dialdehyde, (3-aminopropyl)triethoxysilane, 2,2′-azino-*bis*(3-ethylbenzthiazoline-6-sulfonic acid) (ABTS). Other chemicals used were toluene (J. T. Baker, HPLC grade), absolute ethanol (Pharmco), and hydrogen peroxide (30%, Fluka). Ultrapure water from NANOpure Diamond (Barnstead) source was used in all of the experiments.

Immobilization of enzymes on a solid support: Glass beads (1 mm diameter, Turtle Rainbow®; Portland, OR, USA) were used as solid support for enzyme immobilization. The surface of the beads was cleaned by treatment with piranha solution (25% (*v/v*) of 30% H_2O_2, and 75% (*v/v*) of 98% H_2SO_4) for 30 min, then washed several times with water. (***CAUTION!*** Piranha is a vigorous oxidant. Piranha solution reacts violently with organic solvents and is a skin irritant. Extreme caution should be exercised when handling piranha solution.) Water was removed from the beads by incubation at 40 °C, overnight. The surface of the glass beads was modified by treating them with (3-aminopropyl)triethoxysilane (APTES; 1% (*v/v*) in toluene), overnight at room temperature (23 ± 2 °C). The silanized surface was washed first with toluene and then with ethanol and water to remove unreacted materials. In order to attach GOx covalently, the amino-functionalized surface of the silanized glass beads was treated with glutaric dialdehyde (5%, *v/v*) in phosphate buffer (0.01 M, pH 7.0) for 20 min at room temperature, and then washed several times with phosphate buffer. The glutaric dialdehyde-activated beads were treated with GOx (1 mg mL^{-1}) in phosphate buffer (0.01 M, pH 7.0) for 20 min at room temperature, and then washed several times with phosphate buffer. MP-11 (1 mg mL^{-1}) was covalently bound to the silanized beads in HEPES buffer (50 mM, pH 7.2) in the presence of EDC (1 mM) for 3 h; the MP-11-modified beads were washed several times with water to remove unbound material.

Composition of logic gates and input signals: The AND gate consisted of glucose (0.1 M) and ABTS (0.1 mM) in phosphate buffer (0.01 M, pH 7.0; total volume 1 mL). Soluble GOx (0.15 units) and/or MP-11 (5.4×10^{-7} M) were used as input signals to activate the AND gate. Alternatively, immobilized GOx (about 0.48 nmol on 1200 glass beads) and/or immobilized MP-11 (about 7.5 nmol on 250 glass beads) were used as input signals for the AND gate. The OR gate was composed of ethanol (10 mM), glucose (10 mM), and NAD^+ (0.1 mM) in phosphate buffer (0.01 M, pH 8.2; total volume 1 mL). Soluble GDH (1.5 units) and/or AlcDH (3.14 units) were used as the input signals to activate the OR gate. The XOR gate consisted of ethanol (10 mM), H_2O_2 (1 mM), NADH (0.1 mM), and NAD^+ (0.1 mM) in phosphate buffer (0.01 M, pH 8.2; total volume 1 mL). Soluble AlcDH (5.14 units) and/or MP-11 (5.4×10^{-6} M) were used as the input signals for the XOR gate. The InhibA gate was composed of ethanol (10 mM), H_2O_2 (1 mM), and NADH (0.1 mM) in phosphate buffer (0.01 M, pH 8.2; total volume 1 mL). Soluble AlcDH (6.28 units) and/or MP-11 (5.4×10^{-6} M) were used as the input signals for the InhibA gate. Note that oxygen was present in all solutions (under equilibrium with air), and it was used by GOx upon the biocatalytic oxidation of glucose.

Measurements: The absorbance changes of the OR, XOR, and InhibA logic gates that operated with soluble enzymes as the input signals were measured after a time interval of 5 min following enzyme inputs. The AND gate spectra were measured after 2 min in the case of soluble enzymes, or after 10 min in the case of immobilized enzymes. The concentrations of the substrates (the gates' composition) and the quantities of the enzyme inputs were optimized in order to produce a significant change in $|\Delta A|$; this resulted in a corresponding "0" or "1" state. The reference cuvette was filled with the same composition as the test cuvette prior to the addition of the enzyme inputs; this allowed the differential spectra measurements that corresponded to the changes in the gate composition originating from the enzyme-induced reactions. For the immobilized enzyme inputs, the reactions were performed in separate test tubes upon addition of the glass beads modified with the enzymes. After 10 min of the reaction, the solution was separated from the enzyme-modified glass beads and transferred to the test cuvette for spectral measurements. The presented experimental results and threshold values used represent average data derived from more than ten independent measurements. The absorbance measurements were performed by using a Shimadzu UV-2450PC spectrophotometer. All measurements were performed at $23 \pm 2\,^{\circ}C$.

Tapping mode AFM imaging of the enzymes immobilized on silica wafers was performed by using a Dimension 3100 microscope (Digital Instruments, Inc., Santa Barbara, CA, USA) in ambient conditions. Silicon tips with a radius of 20 nm and resonant frequency of 200–300 KHz were used. For analysis of the AFM data, we used DI Nanoscope software (Digital Instruments). Thicknesses of the biocatalytic thin films grafted onto the APTS layer were measured with a null-ellipsometer (Multiscope, Optrel, Berlin, Germany) by taking into account the known refractive index of the biomaterial.[44] The wavelength of the laser was 632.8 nm. The film thickness was measured at an incident angle of 70°. For data interpretation we used a multilayer model of the grafted films according to the protocol described in the literature.[45]

The amount of GOx immobilized on the glass beads was determined by using hydrolysis of the protein followed by optical analysis of the products.[46] GOx was immobilized on 2000 glass beads by using APTES and glutaric dialdehyde as described above. After washing, the beads were submerged in NaOH (1 M) for 2 h and then neutralized with hydrochloric acid. The solution was measured for absorbance at $\lambda = 280$ nm. The amount of hydrolyzed protein was calculated by using the extinction coefficient of the products obtained upon hydrolysis of GOx, $E\,1\% = 16.7$;[47] this gave the result of in approximately 0.4 pmol protein per bead.

Acknowledgements

This research was supported by the NSF grants "Signal-Responsive Hybrid Biomaterials with Built-in Boolean Logic" (DMR-0706209) and "Biochemical Computing: Experimental and Theoretical Development of Error Correction and Digitalization Concepts" (CCF-0726698).

Keywords: biocomputing · Boolean logic · enzymes · logic gates · molecular devices

[1] A. Adamatzky, B. De Lacy Costello, T. Asai, *Reaction-Diffusion Computers*, Elsevier, Amsterdam, **2005**.
[2] *Unconventional Computing 2005: From Cellular Automata to Wetware* (Eds.: C. Teuscher, A. Adamatzky), Luniver, Beckington, **2005**.
[3] A. P. De Silva, S. Uchiyama, *Nat. Nanotechnol.* **2007**, *2*, 399–410.
[4] U. Pischel, *Angew. Chem.* **2007**, *119*, 4100–4115; *Angew. Chem. Int. Ed.* **2007**, *46*, 4026–4040.
[5] E. Katz, I. Willner, *Angew. Chem.* **2005**, *117*, 4869–4872; *Angew. Chem. Int. Ed.* **2005**, *44*, 4791–4794.
[6] K. Szacilowski, W. Macyk, *Solid-State Electron.* **2006**, *50*, 1649–1655.
[7] R. Baron, A. Onopriyenko, E. Katz, O. Lioubashevski, I. Willner, S. Wang, H. Tian, *Chem. Commun.* **2006**, 2147–2149.
[8] E. Katz, I. Willner, *Chem. Commun.* **2005**, 5641–5643.
[9] A. Credi, V. Balzani, S. J. Langford, J. F. Stoddart, *J. Am. Chem. Soc.* **1997**, *119*, 2679–2681.
[10] F. Pina, M. J. Melo, M. Maestri, P. Passaniti, V. Balzani, *J. Am. Chem. Soc.* **2000**, *122*, 4496–4498.
[11] E. Katz, A. N. Shipway, I. Willner in *Photoreactive Organic Thin Films* (Eds. S. Sekkat, W. Knoll), Academic Press, San Diego, **2002**, pp. 219–268.
[12] L. Li, M. X. Yu, F. Y. Li, T. Yi, C. H. Huang, *Colloids Surf. A* **2007**, *304*, 49–53.
[13] L. Zhao, Q. Hou, D. Sui, Y. Wang, S. Jiang, *Spectrochim. Acta Part A* **2007**, *67*, 1120–1125.
[14] E. Katz, A. N. Shipway in *Bioelectronics: From Theory to Applications* (Eds.: I. Willner, E. Katz), Wiley-VCH, Weinheim, **2005**, pp. 309–338.
[15] S. Vasiliev, M. Pita, E. Katz, *Electroanalysis* **2008**, 20, 22–29.
[16] M. Asakawa, P. R. Ashton, V. Balzani, A. Credi, G. Mattersteig, O. A. Matthews, M. Montalti, N. Spencer, J. F. Stoddart, M. Venturi, *Chem. Eur. J.* **1997**, *3*, 1992–1996.
[17] Y. Zhou, H. Wu, L. Qu, D. Zhang, D. Zhu, *J. Phys. Chem. B* **2006**, *110*, 15676–15679.
[18] F. Pina, A. Roque, M. J. Melo, I. Maestri, L. Belladelli, V. Balzani, *Chem. Eur. J.* **1998**, *4*, 1184–1191.
[19] J. Andreasson, S. D. Straight, G. Kodis, C.-D. Park, M. Hambourger, M. Gervaldo, B. Albinsson, T. A. Moore, A. L. Moore, D. Gust, *J. Am. Chem. Soc.* **2006**, *128*, 16259–16265.
[20] Y. Liu, W. Jiang, H.-Y. Zhang, C.-J. Li, *J. Phys. Chem. B* **2006**, *110*, 14231–14235.
[21] W. Sun, Y.-R. Zheng, C.-H. Xu, C.-J. Fang, C.-H. Yan, *J. Phys. Chem. C* **2007**, *111*, 11706–11711.
[22] J. Andreasson, S. D. Straight, S. Bandyopadhyay, R. H. Mitchell, T. A. Moore, A. L. Moore, D. Gust, *J. Phys. Chem. C* **2007**, *111*, 14274–14278.
[23] D. Margulies, C. E. Felder, G. Melman, A. Shanzer, *J. Am. Chem. Soc.* **2007**, *129*, 347–354.
[24] G. Ashkenasy, M. R. Ghadiri, *J. Am. Chem. Soc.* **2004**, *126*, 11140–11141.
[25] G. Ashkenasy, R. Jagasia, M. Yadav, M. R. Ghadiri, *Proc. Natl. Acad. Sci. USA* **2004**, *101*, 10872–10877.
[26] K. Szaciłowski, *Chem. Eur. J.* **2004**, *10*, 2520–2528.
[27] R. Stadler, S. Ami, C. Joachim, M. Forshaw, *Nanotechnology* **2004**, *15*, S115–S121.
[28] A. P. De Silva, Y. Leydet, C. Lincheneau, N. D. McClenaghan, *J. Phys. Condens. Matter* **2006**, *18*, S1847–S1872.
[29] A. Adamatzky, *IEICE Trans. Electronics* **2004**, *E87C*, 1748–1756.
[30] G. Bell, J. N. Gray in *Beyond Calculation: The Next Fifty Years of Computing* (Eds.: P. J. Denning, R. M. Metcalfe), Copernicus/Springer, NewYork, **1997**, p. 30.
[31] X. G. Shao, H. Y. Jiang, W. S. Cai, *Prog. Chem.* **2002**, *14*, 37–46.
[32] M. N. Stojanovic, D. Stefanovic, T. LaBean, H. Yan in *Bioelectronics: From Theory to Applications* (Eds.: I. Willner, E. Katz), Wiley-VCH, Weinheim, **2005**, pp. 427–455.
[33] R. Unger, J. Moult, *Proteins Struct. Funct. Bioinf.* **2006**, *63*, 53–64.
[34] L. Goncharova, Y. Melnikov, A. O. Tarakanov, *Artif. Immune Syst. Proc. Lect. Notes Comput. Sci.* **2003**, *2787*, 102–110.
[35] M. L. Simpson, G. S. Sayler, J. T. Fleming, B. Applegate, *Trends Biotechnol.* **2001**, *19*, 317–323.
[36] R. Baron, O. Lioubashevski, E. Katz, T. Niazov, I. Willner, *Org. Biomol. Chem.* **2006**, *4*, 989–991.
[37] R. Baron, O. Lioubashevski, E. Katz, T. Niazov, I. Willner, *J. Phys. Chem. A* **2006**, *110*, 8548–8553.
[38] R. Baron, O. Lioubashevski, E. Katz, T. Niazov, I. Willner, *Angew. Chem.* **2006**, *118*, 1602–1606; *Angew. Chem. Int. Ed.* **2006**, *45*, 1572–1576.
[39] T. Niazov, R. Baron, E. Katz, O. Lioubashevski, I. Willner, *Proc. Natl. Acad. Sci. USA* **2006**, *103*, 17160–17163.

[40] *Methods of Enzymatic Analysis, Vol. 3*, 3rd ed., (Ed.: H. U. Bergmeyer), VCH, Weinheim, **1983**, pp. 286–293.
[41] *Methods of Enzymatic Analysis, Vol. 4*, 2nd ed. (Ed.: H. U. Bergmeyer), Academic Press, New York, **1974**, pp. 2066–2072.
[42] F. W. Scheller, F. Schubert, R. Renneberg, H.-G. Müller, M. Jänchen, H. Weise, *Biosensors* **1985**, *1*, 135–160.
[43] Protein Data Bank: http://www.rcsb.org/pdb/home/home.do
[44] J. Benesch, A. Askendal, P. Tengvall, *J. Colloid Interface Sci.* **2002**, *249*, 84–90.
[45] A. Sidorenko, S. Minko, K. Schenk-Meuser, H. Duschner, M. Stamm, *Langmuir* **1999**, *15*, 8349–8355.
[46] H. Sah, *J. Pharm. Sci.* **1997**, *86*, 1315–1318.
[47] G. D. Fasman, *Handbook of Biochemistry and Molecular Biology*, CRC, Boca Raton, **1990**, p. 244.

Received: December 18, 2007
Published online on April 8, 2008

